

RCIC GOVERNING EQUATION SCOPING STUDIES FOR SEVERE ACCIDENTS

Kyle Ross and Jeff Cardoni

Sandia National Laboratories, Albuquerque, NM 87185, USA

kwross@sandia.gov, jncardo@sandia.gov

ABSTRACT

A simplified but mechanistic governing equation for a reactor core isolation cooling (RCIC) system is developed to support investigations into severe accident mitigation strategies. Since the RCIC uses a single-stage impulse turbine, the model is essentially the application of Newton's Laws for a rotational system. Specifically, the control volume formulation of angular momentum conservation is used to derive an equation of motion that is simple enough to be implemented as user input for lumped parameter codes such as MELCOR. Preliminary testing of the RCIC equations and solution methodology has been completed. The equations are integrated into MELCOR input via control functions for scoping calculations; the derivation of the equations and solution methods are intentionally selected to facilitate this effort and the subsequent scoping calculations. The MELCOR model used for the test calculations contains simplified representations of the RCS and RCIC piping for a generic 2000 MW BWR. Scoping calculations of the accident scenario at Fukushima unit 2 are presented that show promising initial results. In conjunction with a literature review of RCIC turbine design, a key conclusion is established that the simplicity and pure-impulse design of the turbine facilitates computational modeling using simplified (lumped-parameter) momentum methods.

KEYWORDS

Severe accident, reactor core isolation cooling, RCIC, impulse turbine

1. INTRODUCTION

The RCIC is a key system for mitigation of severe accidents, as exemplified by the unit-2 accident at Fukushima Daiichi where RCIC delayed core damage for about 70 hours without operator intervention [1-5]. Thus, the RCIC is notionally a resilient and perhaps quasi-passive system that might be counted upon in severe accident management guidelines (SAMGs) to manage decay heat until external pumps and water supplies, dubbed flex equipment/strategies, are employed to stabilize the plant. Technical confidence in RCIC operation under severe conditions hinges upon increased analytical and experimental understanding of the system.

A mechanistic model is therefore required that considers the dynamic forces imparted on the turbine in order to support severe accident research where RCIC operates outside its design envelope. The RCIC uses a pure impulse turbine, so this essentially amounts to applying Newton's Laws for a rotational system where the forces on the turbine include impulses from water and steam, friction losses (windage), shock losses in the buckets, and torque from the pump shaft. The control volume formulation of angular momentum conservation is used to derive an equation of motion for turbine speed that is simple enough to be implemented as user input for lumped parameter codes such as MELCOR. The control volume approach readily lends itself to integration with MELCOR, and allows for easy identification of model parameters that require derivation through other means such as CFD and experimental measurements. Alternatively, these parameters may simply be used as tuning variables through benchmarking against operating data (e.g., Fukushima data and RCIC startup test data). This work presents a literature review of RCIC turbine design, the development of a novel and mechanistic RCIC model, and test calculations of the Fukushima unit 2 accident sequence.

2. RCIC OVERVIEW

An overview of RCIC turbine design is presented here to provide context for the modeling approach. Thorough review of more system-oriented aspects of the RCIC can be found in other sources [6,7]. For this work it is sufficient to note that RCIC is a steam-driven turbine-pump that provides makeup water to the reactor pressure vessel (RPV) following core isolation events. The turbine receives steam from the RPV, via relatively small piping tapped off a main steam line (MSL), which then drives a pump by means of a common shaft. The pump may take suction from the condensate storage tank (CST) or from the wetwell (WW) of the containment. The turbine discharges steam to the wetwell.

The turbine in the RCIC system is a small, single-stage, compound-velocity, impulse turbine [8] originally designed and manufactured by the Terry Steam Turbine Company, which was later purchased by Ingersoll-Rand in 1974. Terry turbines are currently marketed by Dresser-Rand. The turbine is essentially a solid cylindrical wheel with several semi-circular ‘buckets’ that are shaped into the body of the wheel. All Terry RCIC applications in the US use a “G turbine frame size” [8] that denotes a 24 inch (0.61 m) diameter turbine wheel. Fixed nozzles and reversing chambers surround the wheel inside the turbine casing. Figure 1 illustrates the geometry and flow path of steam through the nozzle, turbine buckets, and reversing chambers.

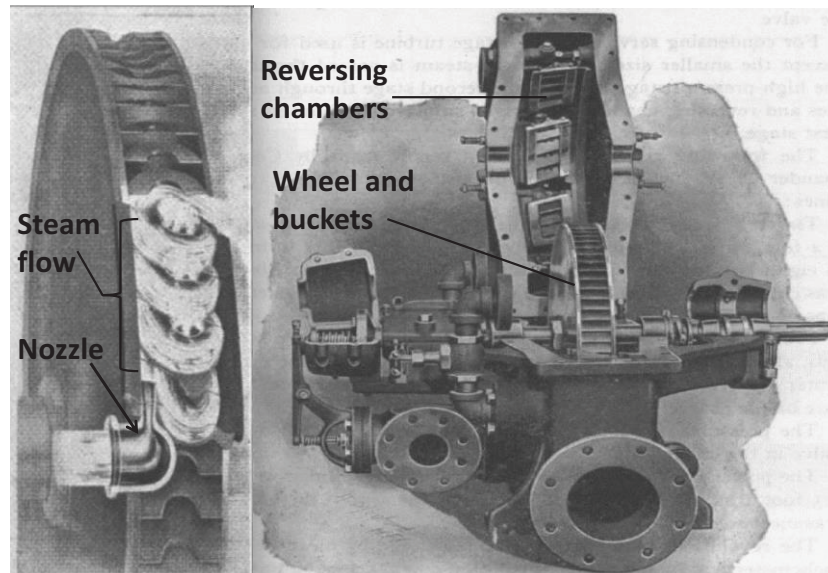


Figure 1. Terry turbine bucket flow (left) and interior view of turbine case (right) [11, 12].

Steam enters the semi-circular buckets after expanding through five to ten nozzles that are fixed around the wheel; steam flow direction is reversed 180° in the buckets. The nozzles are separated by at least three buckets to make room for reversing chambers that also surround the wheel. Since the steam is (almost) completely expanded after exiting the nozzles, which are fixed and detached from the turbine wheel, the expansion process itself imparts no energy on the turbine [9-11]. For this reason, the pressure drop and the enthalpy change over the RCIC turbine are essentially zero. This is in direct contrast to the operation of a reaction turbine where steam expands in the turbine blades, and the blades themselves act as nozzles. Hence, the typical formulas and relationships for multi-stage reaction turbines are not valid for mechanistic analyses of RCIC turbines. Being a pure impulse turbine, RCIC principally operates on the exchange of momentum and kinetic energy. Turbine motion is induced by means of steam acceleration in the buckets after it has been totally expanded through the nozzles.

The compound-velocity feature of the Terry design refers to the fixed reversing chambers that redirect ejected steam back into the buckets several times. The intent is to capture as much of the steam's kinetic energy as possible—steam is typically reversed three to five times at lower turbine speeds before it is fully exhausted through small venting ports in the reversing chambers [8-10]. As shown in Figure 1, the reversing chambers are slightly angled to direct the steam forward (in the direction that the turbine spins) into the downstream buckets.

The fixed reversing chambers in Terry turbines are a proven design feature for lower turbine speeds (typically less than 1300 rpm [9]), but there is considerable evidence that suggests the reversing chambers are of secondary importance for the higher speeds that RCIC operates [9, 10]. An EPRI maintenance manual for RCIC states that the influence of the reversing chambers is minimal for speeds above 2500 rpm [8]. The rated speed of a typical BWR Terry turbine is around 4000-4700 rpm [8]. Therefore, it is reasonable to assume that the reversing chambers are only important for the initial startup of the RCIC. This assumption is physically intuitive upon examination of the Terry turbine geometry: Fluid flow between the buckets and reversing chambers requires proper alignment that probably becomes 'out of phase' when the turbine is at high speed. During startup of the RCIC, the turbine buckets are effectively stationary relative to the steam velocity, and thus there is proper exchange of steam between the buckets and reversing chambers. At rated conditions, the RCIC turbine is designed and sized such that the tangential velocity at the turbine radius (i.e. the "bucket velocity") is about half the steam velocity from the nozzles. Conversely, Terry turbines were originally designed to have a bucket to steam velocity ratio of about 1:8 [10]. The relatively slow bucket velocity of the original Terry designs supports the assertion that the reversing chambers were more important for low speed turbine applications.

The model derivation in Section 3 makes use of the following set of assumptions/assertions that are based on literature review of design, operation, and maintenance of Terry turbines:

- RCIC uses a single-stage Terry impulse turbine that functions according to the exchange of momentum and kinetic energy.
- Steam enters semi-circular buckets and reverses direction ($\sim 180^\circ$).
- The reversing chambers are only important for low speed operation, such as during initial startup.
- The expansion of steam through the nozzles is total; the expansion process converts the static pressure of the steam into kinetic energy to be imparted into the turbine buckets.

3. MODEL APPROACH AND DERIVATION

Rigorous assessment of RCIC operation for a wide range of accident conditions entails the use of a mechanistic model that dynamically considers the forces imparted on the turbine and predicts the integrated behavior of the turbine-pump. The RCIC model must also be amenable to coupling with system-level codes that simulate the thermal-hydraulics of the reactor coolant system (RCS) for long transients (i.e. several days for severe accidents). Such analyses inherently involve large uncertainties, so it is further desirable that the model be simple enough to facilitate fast computation of many different calculations. A lumped-parameter approach is therefore used to derive governing equations for RCIC.

3.1. Governing Equations for RCIC Model

The RCIC governing equation is based on a control volume formulation of the angular momentum equation where the control volume is an enclosure surrounding the turbine buckets that slices through the shaft of the turbine-pump; the nozzles are outside of the control volume. This approach is adapted from Reference [13] for a control volume analysis of a Pelton turbine, which is similar to a Terry turbine in theoretical and design aspects. The turbine responds principally to the impulses of vapor and liquid water that exit the nozzles. A key quantity is thus the momentum flux of the fluid delivered to the turbine

buckets. The momentum flux of the fluid recirculated by the reversing chambers is probably only significant during system startup.

The main impedance to turbine acceleration is resistance from the centrifugal pump. The turbine and pump are connected by a common shaft. Therefore, the turbine speed must equal the pump speed at all times, and the forces resisting the pump are felt instantaneously by the turbine. The pump displaces volume of fluid (water) against head of fluid being pumped, i.e., losses in the RCIC injection piping and RCS and the RPV pressure being pumped against. Other resistance forces on the turbine itself include friction losses (e.g. windage) and so-called shock losses [14] that are the result of fluid streams entering buckets at the wrong angle. Shock losses for the RCIC might be important for high speed operation where the reversing chambers no longer function ideally, especially under two-phase conditions where significant water flashing may disturb the nominal flow patterns. However, these loss mechanisms are currently neglected, and only the first-order forces on the turbine are considered: the fluid impulses in the buckets and the pump resistance.

Equation 1 provides the pertinent scalar component of the angular momentum relationship for a control volume [13]. The turbine is assumed to be adiabatic, which is probably a good approximation for a pure impulse turbine. The turbine only spins in one direction along a stationary axis, which is the θ -coordinate for a cylindrical (r - θ) coordinate system. The control volume for the RCIC turbine is a cylindrical boundary about the wheel and buckets that intersects the shaft. The coordinate system for this control volume is centered at the centroid/axis of the wheel and is stationary; hence the coordinate system is inertial and Equation 1 is valid. An example of a non-inertial configuration would be a turbine inside a system that is accelerating, such as an airplane.

$$\oint r T_{\theta} dA + \iiint r B_{\theta} dV = \oint r u_{\theta} (\rho \mathbf{u} \cdot d\mathbf{A}) + \frac{\partial}{\partial t} \iiint r u_{\theta} \rho dV \quad (1)$$

In Equation 1, r is the radius of the turbine wheel, T_{θ} is a force function over the surface of the control volume (with area A and volume V), B_{θ} is a body force such as gravity, \mathbf{u} is the velocity vector, u_{θ} is the tangential component of the outlet velocity of the fluid leaving the bucket, and ρ is the fluid density. The tangential outlet velocity introduces additional important variables such as the nozzle-bucket inlet and outlet angles, the bucket velocity, and the angular speed of the turbine. These relationships may be resolved using velocity triangles. Appendix A describes how the tangential outlet velocity for the Terry turbine can be written as:

$$u_{\theta} = r\omega - (V_j - r\omega)\cos\beta \quad (2)$$

In Equation 2, ω is turbine speed ($r\omega$ is the bucket speed), V_j is the nozzle jet velocity, and β is the inlet/exit angle between the fluid velocity vectors and the horizontal/tangential direction of the turbine motion (i.e. the bucket velocity vector). This angle is discussed more in Appendix A.

Neglecting minor losses, the only torque that penetrates the boundary of the control volume is the shaft torque. The shaft torque, which is also the pump torque, must be equal and opposite to the torque developed by the fluid action on the turbine according to Newton's Third Law. Thus the first term in Equation 1 may be reduced to:

$$\oint r T_{\theta} dA = -T_{shaft} = -T_{pump} \quad (3)$$

In Equation 3, T_{pump} is the pump torque that is generally a function of other variables including time. The pump torque is discussed more in Section 3.3.

The second term (with B_θ) in Equation 1 is zero because this analysis neglects gravity. For one-dimensional inlets and outlets, the third term in Equation 1 may be rewritten as:

$$\oint ru_\theta(\rho \mathbf{u} \cdot d\mathbf{A}) = \sum_{out} |\mathbf{R} \times \mathbf{u}|_o \dot{m}_o - \sum_{in} |\mathbf{R} \times \mathbf{u}|_{in} \dot{m}_{in} \quad (4)$$

Equation 4 shows that this term represents the driving moment of the fluid flow in the buckets. The evaluation of this term for one-dimensional inlets and outlets is commonly demonstrated in introductory textbooks on fluid mechanics (e.g. [13][15]). For the RCIC model, the cross products in Equation 4 can be simplified upon consideration of the Terry turbine geometry. For the Pelton turbine problem from Reference [13], where the fluid inlet and out velocities are parallel to the bucket velocity, Equation 4 reduces to:

$$\oint ru_\theta(\rho \mathbf{u} \cdot d\mathbf{A}) = ru_\theta \dot{m} - rV_j \dot{m} = r\dot{m}(u_\theta - V_j) \quad (5)$$

Equation 5 is the difference between the moments of outlet and inlet momentum fluxes for the Pelton turbine, multiplied by the effective outlet and inlet flow areas. This equation neglects losses in the bucket and assumes that the bucket inlet and outlet mass flow rates are identical (given by \dot{m}), which reflects mass conservation for the bucket. The mass flow rates through the bucket are assumed to be the same as the mass flow rate exiting the nozzle. Hence at any given time it is assumed that $\dot{m}_{nozzle} = \dot{m}_{bucket}$ and the bucket velocities can be resolved using simple velocity triangles. The details of such pseudo-steady assumptions for the bucket flow may be revised pending CFD and experimental analyses of the RCIC.

The fluid velocities for the Terry turbine are not parallel to the bucket velocity. The fluid enters the buckets from the nozzles at an angle that effectively reduces the moment arm of the momentum flux. From a design perspective, the reduced moment-arm is probably compensated for by the increased number of buckets and nozzles that can fit around the wheel for the Terry configuration. Figure A.1 and Figure A.2 in Appendix A demonstrate this velocity orientation for the Terry turbine. Thus, Equation 4 and Equation 5 can be modified for the Terry geometry to become:

$$\oint ru_\theta(\rho \mathbf{u} \cdot d\mathbf{A}) = r\dot{m}(u_\theta - V_j \cos\beta) \quad (6)$$

Substituting the formula for u_θ (Eq. 2) into Equation 6 yields the following expression:

$$\oint ru_\theta(\rho \mathbf{u} \cdot d\mathbf{A}) = r^2 \dot{m} \omega (1 + \cos\beta) - 2r\dot{m}V_j \cos\beta \quad (7)$$

Using Equations 1, 2, 3, and 7, the original governing equation can now be written as:

$$-T_{pump} = r^2 \dot{m} \omega (1 + \cos\beta) - 2r\dot{m}V_j \cos\beta + \frac{\partial}{\partial t} \iiint r(r\omega - (V_j - r\omega)\cos\beta)\rho dV \quad (8)$$

Further formulation from this point depends on the implementation scheme into the thermal-hydraulic code. Two possible schemes are developed and described in Section 3.2. and Section 3.3.

3.2. Quasi-steady Scheme

Severe accident transients for LWRs, such as those at Fukushima unit 2, are rather slowly evolving with respect to time. There are often time periods where important variables such as RPV pressure only change by about 1-10% over the course of several hours. Hence it is reasonable to presume that a quasi-steady form of the RCIC equation may be used to gradually ‘steer’ the transient thermal-hydraulic calculation. This neglects turbine-pump inertia and forces the RCIC to make instantaneous changes between quasi-equilibrium conditions every time the RCIC inputs (i.e. the momentum and mass fluxes) are updated by

the thermal-hydraulic code; the frequency of the input updating is the coupling time step, which is currently set to be every thermal-hydraulic time step in this work.

The time derivative in Equation 8 is zero for the quasi-steady scheme. Therefore the angular momentum equation reduces to:

$$T_{pump} = 2r\dot{m}V_j \cos\beta - r^2\dot{m}\omega(1 + \cos\beta) \quad (9)$$

The instantaneous power developed by the pump is equal to the product of pump torque and angular speed; pump power is also equal to the product of the head (h) and volumetric flow rate (Q) of the pump. Equation 10 can then be used to relate the pump torque to the pump head.

$$\text{Power} = T\omega = hQ. \quad (10)$$

The pump torque relationship from Equation 9 can be inserted into Equation 10 and then solved for the pump head. This formula pump head can implemented directly as input for common system thermal-hydraulic codes such as MELCOR.

Upon implementing the pump head formula into a MELCOR model, the relationship is expanded to consider the flow of two phases. The effects of steam and water jetting from the turbine drive nozzles and impinging on the turbine wheel are assumed to be fully distinct and additive in that separate mass flow rate and velocity terms are included for each of the phases in Equation 9. In reality there may be important joint influences. Flashing of the liquid and/or condensation of the vapor may be important. MELCOR's flashing model is employed at the nozzles to capture first order deleterious effects of liquid flashing as it exits the nozzles, but this is an area where CFD investigations are expected to contribute important realism.

The pump head formula for two-phase flow that is incorporated into the MELCOR test problem in Section 4 is given by Equation 11, where v subscripts denote vapor flow and l subscripts denote liquid flow.

$$h = \frac{\eta(\omega, Q)}{Q} [2r\omega(\dot{m}_v V_v + \dot{m}_l V_l) \cos\beta - r^2\omega^2(\dot{m}_v + \dot{m}_l)(1 + \cos\beta)]. \quad (11)$$

Equation 11 introduces a parameter η for the pump efficiency, which is generally a function of both the pump speed and the volumetric flow rate (Q) developed by the pump. This term is evaluated using common relationships for centrifugal pumps. Upon implementation into MELCOR, Equation 11 is updated every MELCOR time step. In Equation 11, r and β are true constants, while the fluid velocities and mass flow rates are calculated by the thermal-hydraulic code, as is the pump volumetric flow rate. Because a differential equation is not being solved for the turbine speed, ω must be updated after evaluation of Equation 11. Likewise, the current time step solution of Equation 11 uses an 'old' value for ω . Turbine speed is calculated according to Equation 12, where ω_{rated} and h_{rated} are model input parameters for the rated pump speed and pump head.

$$\omega = \omega_{rated} \sqrt{\frac{h}{h_{rated}}}. \quad (12)$$

3.3. Time-dependent differential equation scheme

The quasi-steady approach in Section 3.2 neglects the inertia of the turbine-pump. Even though LWR severe accidents generally evolve slowly with time, there are likely certain time periods that would benefit from the use of a differential equation for turbine speed. For instance, the unit 2 accident sequence

exhibits several time periods where the effects of turbine-pump inertia may be important; these include RCIC startup (near 1 hour after scram), the onset of two-phase flow into the RCIC (unknown timing), the pump suction switch from the CST to the WW (near 13 hours), and eventual system failure near 68 hours after reactor shutdown [1].

Equation 8 can be written as:

$$-T_{pump} = r^2 \dot{m} \omega (1 + \cos \beta) - 2r \dot{m} V_j \cos \beta + I(1 + \cos \beta) \frac{d\omega}{dt} \quad (13)$$

The time derivative term from Equation 8 has been replaced with $I(1 + \cos \beta) \frac{d\omega}{dt}$, where I is the turbine moment of inertia. Appendix B shows the derivation of this term. Equation 13 can be rearranged as:

$$I \frac{d\omega}{dt} + r^2 \dot{m} \omega (t) = \frac{-T_{pump}(t)}{1 + \cos \beta} + 2r \dot{m} V_j \frac{\cos \beta}{1 + \cos \beta} \quad (14)$$

Equation 14 is a first-order differential equation for turbine speed. If the pump torque was a known function and the coefficients were constants or functions of time only, then this equation would be readily solvable by Laplace transformation. Since this is not the case, a constitutive relationship is necessary to solve the equation. Centrifugal pump torque is proportional to the pump speed squared. Therefore the pump torque can be expressed as:

$$T_{pump}(t) = \eta(\omega(t), Q) \frac{T_o}{\omega_o^2} \omega^2(t) \quad (15)$$

In Equation 15, η is an efficiency term that is currently treated as the same pump efficiency defined for the pump head in Equation 11. In general, these two efficiencies may not be identical, but this assumption is deemed sufficient for this scoping study. T_o and ω_o are the rated pump torque and speed, respectively. After putting Equation 15 into Equation 14, the final differential equation for turbine speed becomes:

$$I \frac{d\omega}{dt} + r^2 \dot{m} \omega (t) = -\frac{\eta}{1 + \cos \beta} \frac{T_o}{\omega_o^2} \omega^2(t) + 2r \dot{m} V_j \frac{\cos \beta}{1 + \cos \beta} \quad (16)$$

It is noted that the same differential equation for turbine speed could be derived directly from the cross product of Newton's Second Law (i.e. $\frac{d\mathbf{p}}{dt} = \sum \mathbf{F}$). This is consistent with the fact that the angular momentum equation is obtained from the cross product of the linear momentum equation, which is also a statement of Newton's Second Law. The familiar formula is $I \frac{d\omega}{dt} = \sum M$. The evaluation of this equation simply requires careful consideration of the appropriate signs and angles for the various terms that comprise $\sum M$, the summation of moments acting on the turbine.

The only true constants in Equation 16 are I , r , and β . The other terms are generally functions of several other variables. If these terms were constant or simply functions of time, Equation 16 would be a Riccati equation and an analytical solution might be possible. However, a simple time-discretization scheme is sought for the scoping calculations that can be advanced each time step in unison with a thermal-hydraulic code. The simplest coupling method between the RCIC equation and the thermal-hydraulic code is an explicit scheme where \dot{m} , V_j , and η are assumed to be constant between each coupling time step. Thus the equation can be advanced/integrated quite simply over each time step; this simplistic method is deemed adequate for the current scoping analyses and it will be improved in future work.

An example numerical solution is given here by assuming that \dot{m} , V_j , and η can be treated as pseudo-constants over each integration step—these terms are updated each time step by MELCOR for the test calculations in Section 4. A simple backward (implicit) Euler scheme is derived by the following time-discretization of Equation 16, where Δt is the MELCOR time step size (alternatively it could be a coupling time step):

$$I \frac{\omega_{n+1} - \omega_n}{\Delta t} + r^2 \dot{m} \omega_{n+1} = - \frac{\eta}{1 + \cos\beta} \frac{T_o}{\omega_o^2} \omega_{n+1}^2 + 2r\dot{m}V_j \frac{\cos\beta}{1 + \cos\beta} \quad (17)$$

Equation 17 is a quadratic equation for ω_{n+1} , the new time step value of the turbine speed. Given the simplicity of this equation and the fact that it only models a single computational node, Equation 17 can be solved directly by the quadratic formula.

The implicit Euler solution for ω_{n+1} is given by Equation 18 and it depends on the previous time step value for turbine speed, ω_n . Hence for $n = 1$, ω_1 is the known initial condition and taken to be zero. The negative solution to the quadratic equation is neglected because it would yield negative turbine speeds, and this analysis only considers turbine motion in the positive direction.

$$\omega_{n+1} = \frac{-(I + r^2(\dot{m}_v + \dot{m}_l)\Delta t) + \sqrt{(I + r^2(\dot{m}_v + \dot{m}_l)\Delta t)^2 + 4 \frac{\eta\Delta t}{1 + \cos\beta} \frac{T_o}{\omega_o^2} [I\omega_n + 2r\psi(\dot{m}_v V_v + \dot{m}_l V_l)\Delta t]}}{2 - \frac{\eta\Delta t}{1 + \cos\beta} \frac{T_o}{\omega_o^2}} \quad (18)$$

The mass flow rate and momentum flux terms in Equation 18 have been expanded to include distinct terms for the liquid (subscript l) and vapor (subscript v) phases, as was done in the quasi-steady scheme (see Equation 11). For the differential equation scheme, the pump head quantity that couples to MELCOR is determined using Equation 12 in conjunction with the turbine speed from Equation 18. The angle ratio from Equation 18 is replaced by the constant variable $\psi = \frac{\cos\beta}{1 + \cos\beta}$ for brevity.

4. TEST CALCULATIONS

The RCIC governing equations are tested in a simplified MELCOR model of a generic 2000 MWt BWR. MELCOR is used to simulate the thermal-hydraulic behaviors of the RPV and the two-phase flow through the RCIC steam piping. Because the RCIC turbine discharges steam to the wetwell, which is at a much lower pressure than the RPV, MELCOR must also model two-phase choked flow (as appropriate) at the turbine nozzles and the governor valve. The turbine dynamics are resolved using control functions (i.e. user-formulas that the code calculates each time step) containing the equations from Section 3. In this test model the turbine discharge flow to the wetwell is not modeled (although it could be), and hence the wetwell pressure must be imposed as a boundary condition. The wetwell pressure is most important in determining the wetwell pool temperature if CST-WW switchover is assumed to occur. If the wetwell pressure is known, the pool temperature can be resolved if saturated conditions are also assumed.

4.1. MELCOR Nodalization and RCIC Model Inputs

The MELCOR model has a basic nodalization of the RPV and RCIC piping. The model has seven active control volumes: The RPV is a single control volume; two volumes are between the RPV and the governor valve for the RCIC steam piping; one volume is between the governor valve and the nozzles to represent the RCIC steam chest, which is actually inside the turbine casing; and three volumes are used to model the pump and its piping. The main steam lines are not represented, and the steam piping from the RPV to the turbine is at a constant elevation. The RCIC turbine is a time-independent volume that sees the wetwell pressure. These model simplifications are chosen intentionally in order to expedite the testing

of the RCIC equations and to demonstrate that the model can predict key features of the Fukushima unit 2 accident—a crucial goal in this process is the demonstration of physically reasonable feedback between the RPV and the RCIC under SBO-conditions comparable to Fukushima unit 2, i.e., where the RCIC overfills the RPV and a two-phase mixture spills over into the steam piping leading to the RCIC. A schematic of the RPV-RCIC coupling and feedback is given by Figure 2.

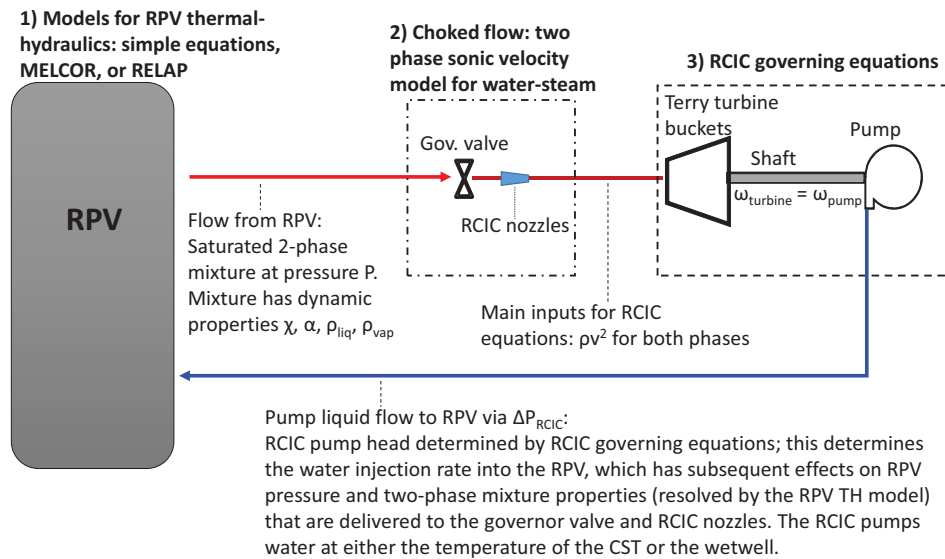


Figure 2. Coupling to be demonstrated by the MELCOR test model.

A summary of the main inputs and boundary conditions employed in the test calculations is given by Table I. The Fukushima test calculations use plant data of containment pressure in order to grossly model the CST-WW switchover. The temperature of the wetwell pool is likely considerably higher than the CST temperature, and this has strong impacts on the RPV thermal-hydraulic response after the switch in pump suction. MELCOR inherently treats the nozzles as converging nozzles that yield choked flow at the throats. In reality the nozzles appear to be of converging-diverging design that could involve supersonic flow near design conditions. The calculations in Section 4.2 predict choked flow at the turbine nozzles and assume that fluid enters the turbine buckets with velocities predicted by MELCOR's models for two-phase critical flow. MELCOR also considers liquid flashing through the nozzles in this process.

Table I. Input values for test calculations

Input variable	Value
Turbine radius (r)	0.3 m (12")
Nozzle inlet/outlet angle ($\alpha=\beta$, see App. A)	$\pi/4$ radians
Nozzle width (square nozzle assumed)	0.01 m (0.39")
Number of nozzles	5
Turbine momentum of inertia (I)	10 kg m ² (237 lb ft ²)
Rated RCIC speed (ω_{rated} , ω_o)	4300 rpm
Rated pump head (h_{rated})	7.52 MPa (1090 psi)
Rated pump torque (T_o)	449 N m (331 lb ft)
Pump injection flow area	0.0168 m ² (0.18 ft ²)
CST-WW suction switch	14 hours
WW pool temperature at switch	387 K

4.2. Test Results for Fukushima-type Accident Scenario

The MELCOR model and RCIC equations are tested using an accident scenario that is comparable to Fukushima unit 2. No ‘tuning’ or rigorous benchmarking against data is attempted here. There are still too many unknown and uncertain model parameters (e.g. bucket angles and velocity coefficients) for such an effort to be meaningful. Moreover, the available plant data is very sparse. The test calculations are instead deliberately performed for a non-Fukushima model to demonstrate that the models have not just been forced to agree with the Fukushima data. For example, the model has an arbitrary power level of 2000 MW and boiler properties from SNL’s Peach Bottom SOARCA model [1], including relatively high safety relief valve (SRV) setpoints (Peach Bottom is a larger 3500 MW reactor).

The test calculation is an extended station blackout where reactor scram occurs at $t = 0$. The only credited safety systems are RCIC and the automatic SRV operation. After $t = 1$ hour, the RCIC is allowed to run uninhibited by any controllers (i.e. no operator throttling or automated trips); its behavior is resolved entirely from the RCIC equations from Section 3 and the MELCOR thermal-hydraulic calculations. The calculation assumes that the governor valve is opened fully at 1 hour and all water injection by the RCIC pump flows to the RPV—no water is diverted back to the CST or wetwell. The RCIC pump initially takes suction from the CST, which has a water temperature of about 289 K, and switchover to the WW is assumed to occur at 14 hours in the test calculations. At this time, the WW pool water is assumed to have a temperature of 387 K. Thus the switchover manifests itself as a sudden and large increase in the water temperature that is injected into the RPV by the RCIC.

Figure 3 shows RPV pressures calculated by the MELCOR/RCIC model compared to the plant data for Fukushima unit 2. The models are predicting key features of the RPV pressure trend that are in reasonable, qualitative agreement with the plant data, despite the simple nature of the MELCOR model and the deliberate modeling of a non-Fukushima reactor. The first drop in RPV pressure in the models from 2-4 hours is the result of the RPV filling rapidly due to full RCIC operation, which is more than capable of handling the decay heat and refilling the vessel especially with the governor valve fully opened and no recirculation of injection water. RPV overfill is typically prevented either by operator throttling (e.g. recirculation of water back to the CST or wetwell via the test and recirculation lines) or by automatic high-level detection that trips the RCIC, neither of which are included in the Fukushima test calculations. During the first hour of the unit 2 accident, the RCIC was started and stopped at least two times, possibly due to high level and manual restarts, and the operators may have throttled injection before they lost all power due to the tsunami. The operators had restarted RCIC just before the tsunami arrived, after which they lost control of it and it appears to have run until at least 66 hours after scram. The calculations corroborate the notion that the system may have operated in a self-regulating fashion for most of this time period.

The calculations predict complete RPV flooding to the MSL elevation near 3 hours. After the RPV water level reaches the MSL elevation, significant saturated water is ingested by the turbine and void fraction at the nozzles decreases (Figure 4), which results in an immediate reduction in RCIC speed (Figure 5) and a sharp increase in RPV pressure back to the SRV setpoint. This trend is mainly the result of decreasing sonic velocity at the nozzles due to increased liquid content in the two-phase mixture. In general, the critical velocity for saturated water and steam (a two-phase, one-component system) decreases with increasing liquid fraction as the mixture expands through a nozzle. Thus, the momentum flux that drives the turbine (Figure 6) decreases considerably. The increased fluid density of the liquid is not as important since momentum flux is proportional to the square of the velocity.

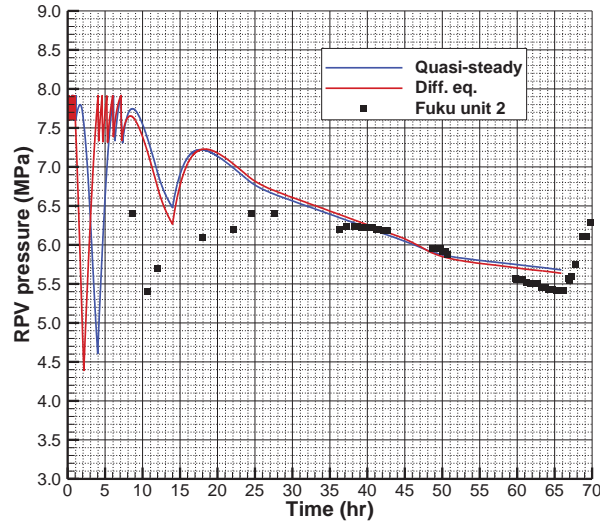


Figure 3. RPV pressure for MELCOR/RCIC models and Fukushima plant data.

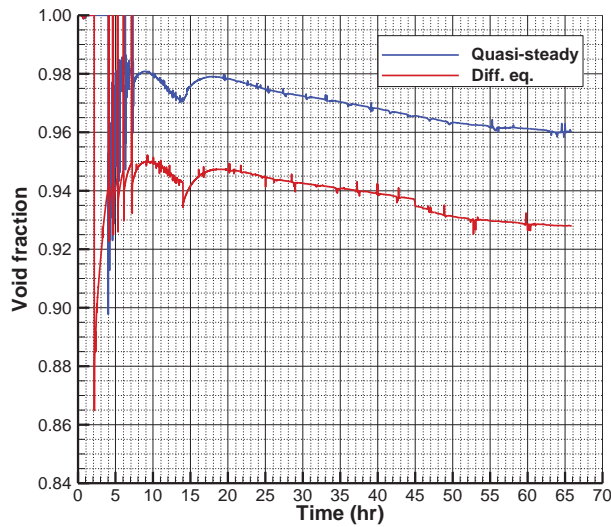


Figure 4. Void fraction into turbine nozzles for MELCOR/RCIC models.

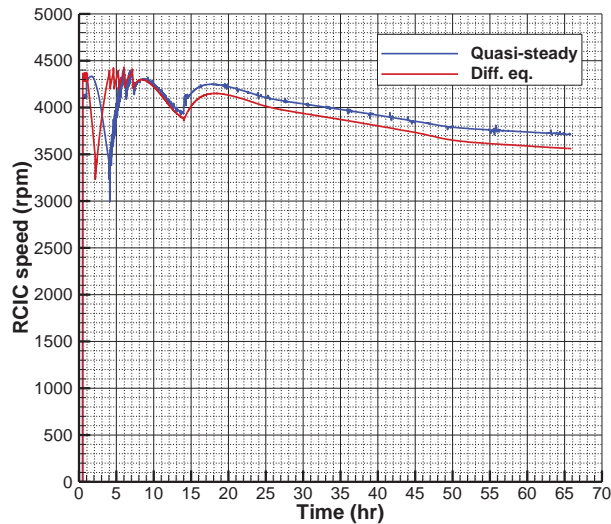


Figure 5. RCIC speed for MELCOR/RCIC models.

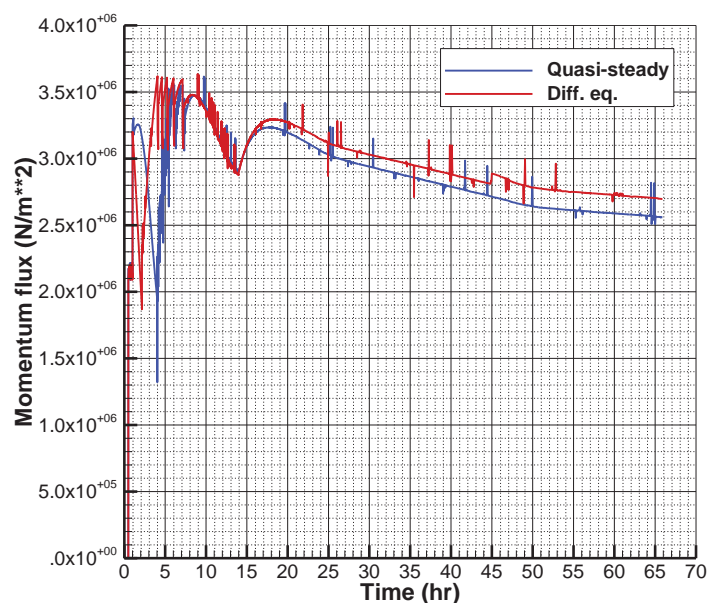


Figure 6. Momentum flux for MELCOR/RCIC models.

In conjunction with decreasing decay heat, a few hours of SRV cycling and RCIC operation causes the steam generation rate in the RPV to decrease enough for pressure to drop below the setpoint near 8 hours. RPV pressure continues to decrease until the CST-WW switchover. The sudden injection of hotter water from the wetwell (+100 K relative to the CST) drives an increase in steam generation rate in the RPV at 14 hours. With less subcooling of the injected water, less energy is required to bring the water to the saturation temperature and more energy is used for steam generation that drives the increase in RPV pressure. Afterwards, the higher RPV pressure increases the steam content of the two-phase mixture at the nozzles (Figure 4), thereby accelerating the RCIC (Figure 5 and Figure 6), which suppresses further pressure rise. The acceleration of the RCIC injects more water into the RPV, which subsequently repeats the feedback process of higher liquid content, degraded momentum flux, reduced RCIC speed, and hence reduced injection into the RPV; the system essentially returns to the state it was in before the CST-WW switchover. This is a vital demonstration of system feedback between the RPV and RCIC. The Fukushima data reveals a comparable trend but the switch in pump suction may have occurred earlier at unit 2.

5. SUMMARY

A mechanistic approach for lumped-parameter modeling of the RCIC has been developed for evaluation of RCIC behavior during severe accidents. Preliminary calculations have been performed that show promising initial results. The calculations demonstrate that the RCIC models have the capability to predict feedback between the RPV and RCIC for severe accidents without operator action. The results provide physical evidence that the RCIC may operate in a self-regulated regime for many hours, and this assertion agrees with the current state-of-knowledge for Fukushima unit 2.

The initial model results are encouraging but leave room for future development and improvement. The accuracy of a lump-parameter model is inherently dependent on the proper definition and quantification of several model parameters that require experimental derivation or computational models with higher spatial fidelity (i.e. CFD). Therefore, future SNL research entails CFD and experimental efforts to complement the system-level models developed in this work. The results from Section 4 also suggest that the numerical coupling between the RCS and RCIC has room for improvement. These results used a simple (explicit) coupling scheme between the models, since the RCIC equations are merely input into the

MELCOR model via control functions. Future efforts will investigate various implicit computational schemes in order to enhance model precision.

ACKNOWLEDGMENTS

Chisom Wilson of SNL is acknowledged for developing the CAD models for the RCIC turbine. Vince Mousseau of SNL is acknowledged for providing valuable insights on the modeling of two-phase flow for turbo-pumps. This work was funded by the US Department of Energy. Sandia National Laboratories is a multi-program laboratory managed and operated by Sandia Corporation, a wholly owned subsidiary of Lockheed Martin Corporation, for the U.S. Department of Energy's National Nuclear Security Administration under contract DE-AC04-94AL85000.

REFERENCES

1. R.O. Gauntt et al., "Fukushima Daiichi Accident Study," SAND2012-6173, Sandia National Laboratories: Albuquerque, NM, USA (2012).
2. Y. Yamanaka, et al. "Update of the First TEPCO MAAP Accident Analysis of Units 1, 2, and 3 at Fukushima Daiichi Nuclear Power Station," *Nuclear Technology*, **186** (2), pp. 263-279 (2014).
3. TEPCO Press Release, "TEPCO Issues Progress Report on Inquiry into Unanswered Details of Fukushima," http://www.tepco.co.jp/en/press/corp-com/release/2014/1240140_5892.html (2014).
4. Tokyo Electric Power Company, "Fukushima Nuclear Accident Analysis Report," available at http://www.tepco.co.jp/en/press/corp-com/release/betu12_e/images/120620e0104.pdf (2012).
5. K.W. Ross et al., "Interim MELCOR Simulation of the Fukushima Daiichi Unit 2 Accident Reactor Core Isolation Cooling Operation," SAND2013-9956, Sandia National Laboratories: Albuquerque, NM, USA (2013).
6. Nuclear Regulatory Commission, "Boiling Water Reactor (BWR) Systems," available at <http://www.nrc.gov/reading-rm/basic-ref/teachers/03.pdf>.
7. General Electric, "General Electric Systems Technology Manual, Chapter 2.7, Reactor Core Isolation Cooling System," available at <http://pbadupws.nrc.gov/docs/ML1125/ML11258A311.pdf>.
8. J. Kelso et al., "Terry Turbine Maintenance Guide, RCIC Application," EPRI Technical Report, report number 1007460, Electric Power Research Institute, Palo Alto, CA, USA (2012).
9. G.A. Orrok, "Small Steam Turbines," *Transactions of the American Society of Mechanical Engineers*, Washington D.C., May 1909, Vol. 31, pp. 263-287 (1910).
10. W.J.A. London, "A Commercial Analysis of the Small-turbine Situation," *Transactions of the American Society of Mechanical Engineers*, New York, December 1917, Vol. 39, pp. 263-287 (1918).
11. C.W. Dyson, "Test of Terry Steam Turbine," *Journal of the American Society of Naval Engineers*, **21** (3), pp. 884-890 (1909).
12. Author Unknown, "The Terry Turbine-Driven Fans," *Journal of the American Society of Naval Engineers*, **30** (3), pp. 598-599 (1918).
13. I.H. Shames, *Mechanics of Fluids*, pp. 156-166, McGraw-Hill Inc., New York, NY, USA (1982).
14. D.A. Mooney, *Introduction to Thermodynamics and Heat Transfer*, pp. 293-296, Prentice Hall Inc., Edgewood Cliffs, NJ, USA (1955).
15. F.M. White, *Fluid Mechanics*, pp. 167-172, McGraw-Hill Inc., New York, NY, USA (2003).

APPENDIX A: Velocity Triangles for Terry Turbine Buckets

A velocity vector analysis of the turbine buckets is necessary to characterize the RCIC system using a lumped-parameter approach. The angular momentum equation that determines the RCIC turbine motion depends on the tangential component of the outlet velocity; this quantity must be resolved from the nozzle jet velocity and the flow angles of the bucket. Figure A.1 depicts velocity triangles for one-way flow through an arbitrarily shaped bucket. The solid arrows with bold variable names represent velocity

vectors, and the dotted lines represent the scalar components of these vectors. Red lines with '1' subscripts are for the inlet flow, and blue lines with '2' subscripts represent the outlet flow. The 'z' variables represent the axial components of the flow velocities, which are not in the imposed direction of the turbine motion. The 'y' variables signify horizontal (i.e. tangential, radial) components of the velocities, which are in the direction of turbine motion (i.e. the same direction as the bucket velocity). Because the bucket is also in motion, the y-components of the velocity have absolute magnitude with respect to the coordinate system and relative magnitude (subscript 'r') with respect to the bucket velocity. Since the bucket width is small compared to the radius of the turbine, the bucket velocity is the same at the inlet and outlet. Figure A.2 shows the approximate placement of the relative fluid velocities as they enter a preliminary CAD model of the Terry turbine.

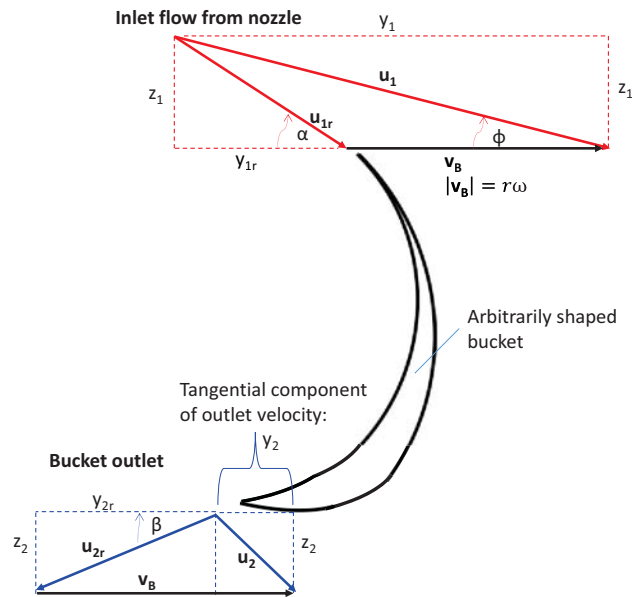


Figure A.1. General velocity diagram for one-way flow in an arbitrary impulse bucket.

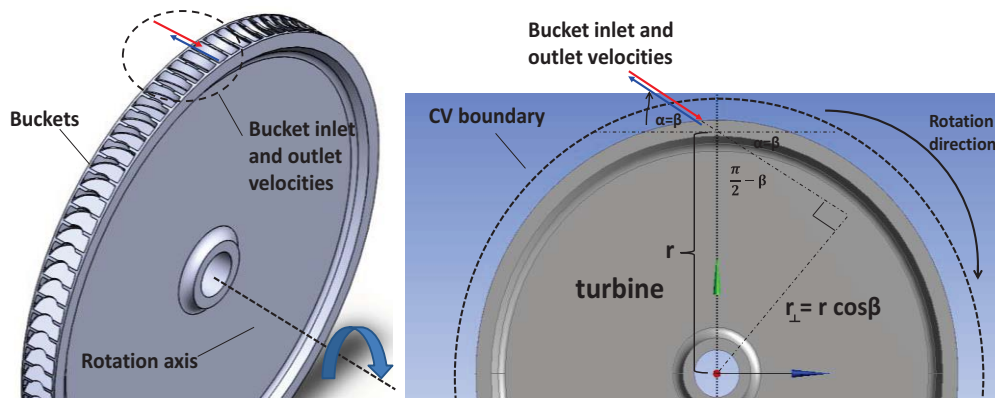


Figure A.2. Orientation of flow velocities for Terry turbine.

There are a few pertinent relationships that are necessary to resolve the tangential component of the outlet velocity (y_2 in Figure A.1 and u_θ in Equation 1). These formulas are simple trigonometry expressions based on Figure A.1 and statements of the known input conditions for the problem. The formulas for the bucket inlet are:

$$|u_1| = V_j, \text{ the jet velocity magnitude} \quad (\text{A.1})$$

$$|\mathbf{v}_B| = r\omega, \text{ the bucket velocity magnitude} \quad (\text{A.2})$$

$$\alpha \approx \beta, \text{ angle between relative inlet/outlet velocities and bucket velocity} \quad (\text{A.3})$$

$$\phi = \text{angle between absolute inlet velocity and bucket velocity} \quad (\text{A.4})$$

$$y_1 = |\mathbf{u}_1| \cos\phi \quad (\text{A.5})$$

$$y_{1r} = y_1 - |\mathbf{v}_B| \quad (\text{A.6})$$

$$|\mathbf{u}_{1r}| = |\mathbf{u}_1 - \mathbf{v}_B| = \sqrt{z_1^2 + y_{1r}^2} = \sqrt{(|\mathbf{u}_1| \sin\phi)^2 + (y_1 - |\mathbf{v}_B|)^2} \quad (\text{A.7})$$

Using the relationship $\sin^2 x + \cos^2 x = 1$ and the assumption that $\cos\phi \approx 1$, Equation A.7 reduces to:

$$|\mathbf{u}_{1r}| = \sqrt{V_j^2 - 2r\omega V_j + r^2\omega^2} = |V_j - r\omega| \quad (\text{A.8})$$

The Terry turbine has roughly equivalent inlet (α) and outlet (β) bucket angles. Preliminary CAD models suggest that this angle may be near 45 degrees ($\pi/4$ radians). The assumption that $\cos\phi \approx 1$ is reasonable considering the magnitude of the V_j and the fact that the bucket speed is on the same order of magnitude of the jet speed at rated conditions. It is also known that the system is designed such that V_j is always larger than the bucket speed ($r\omega$); hence $V_j - r\omega$ is always greater than zero.

The bucket outlet relationships are:

$$|\mathbf{u}_{2r}| = C_B |\mathbf{u}_{1r}| \quad (\text{A.9})$$

$$y_{2r} = |\mathbf{u}_{2r}| \cos\beta \quad (\text{A.10})$$

$$y_2 = |\mathbf{v}_B| - y_{2r} \quad (\text{A.11})$$

C_B is the bucket velocity coefficient. The approximation of $C_B = 1$ is sufficient for the scoping analyses. It is now possible to solve for y_2 , the tangential component of the outlet velocity (i.e. u_θ in Equation 1):

$$y_2 = r\omega - (V_j - r\omega) \cos\beta \quad (\text{A.12})$$

APPENDIX B: Time-derivative in Angular Momentum Equation

This appendix shows that $\frac{\partial}{\partial t} \iiint r u_\theta \rho dV = \frac{\partial}{\partial t} \iiint r(r\omega - (V_j - r\omega) \cos\beta) \rho dV = I(1 + \cos\beta) \frac{d\omega}{dt}$.

First, the integral is expanded:

$$\begin{aligned} \frac{\partial}{\partial t} \iiint r(r\omega - (V_j - r\omega) \cos\beta) \rho dV &= \frac{\partial}{\partial t} \iiint (r^2\omega(t) - rV_j \cos\beta + r^2\omega(t) \cos\beta) \rho dV \\ &= \frac{\partial}{\partial t} \iiint r^2(1 + \cos\beta) \omega(t) \rho dV - \frac{\partial}{\partial t} \iiint rV_j \cos\beta \rho dV \\ &= (1 + \cos\beta) \frac{d\omega}{dt} \iiint \rho r^2 dV + (1 + \cos\beta) \omega(t) \frac{d}{dt} \iiint \rho r^2 dV \end{aligned}$$

Defining the moment of inertia to be $I = \iiint \rho r^2 dV$, which is treated as a constant (hence its time derivative is zero), it is apparent that:

$$\frac{\partial}{\partial t} \iiint r(r\omega - (V_j - r\omega) \cos\beta) \rho dV = I(1 + \cos\beta) \frac{d\omega}{dt}$$

Notionally $I = \iiint \rho r^2 dV$ would represent the moment of inertia of the fluid in the control volume. However, in these scoping analyses it is used to represent the total moment of inertia of the turbine and the fluid in the buckets.